Solar Energy Materials & Solar Cells 94 (2010) 1803–1808

Contents lists available at ScienceDirect

Solar Energy Materials & Solar Cells

journal homepage: www.elsevier.com/locate/solmat

Donor–acceptor conjugates-functionalized zinc phthalocyanine: Towards broad absorption and application in organic solar cells

Fushun Liang [a,*], Fan Shi [a], Yingying Fu [b], Lifen Wang [a], Xintong Zhang [c], Zhiyuan Xie [b,*], Zhongmin Su [a]

[a] Department of Chemistry, Northeast Normal University, Changchun 130024, China
[b] State Key Laboratory of Polymer Physics and Chemistry, Changchun Institute of Applied Chemistry, Chinese Academy of Sciences, Changchun 130022, China
[c] Key Laboratory for UV-Emitting Materials and Technology of Ministry of Education, Northeast Normal University, Changchun 130024, China

ARTICLE INFO

Article history:
Received 16 February 2010
Received in revised form
24 May 2010
Accepted 25 May 2010
Available online 9 June 2010

Keywords:
Zinc phthalocyanine
Donor–acceptor conjugates
Broad absorption
Organic solar cells

ABSTRACT

New zinc phthalocyanine (**ZnPc-TDA**), peripherally functionalized with donor–acceptor conjugates was synthesized, and its optical, thermal, electrochemical, and photovoltaic properties were studied. The black **ZnPc-TDA** exhibited both excellent solubility in common organic solvents, and broad absorption covering the range 300–900 nm. The photovoltaic devices with the configuration of ITO/PEDOT-PSS/**ZnPc-TDA**:PCBM/LiF/Al produced short circuit current densities of 2.26 mA/cm^2, the open circuit voltage of 0.68 V and power conversion efficiency of 0.4% under AM1.5G illumination.

1. Introduction

Harvesting energy directly from sunlight using photovoltaic cells is recognized worldwide as an important solution to the growing energy crisis and environmental pollution. The utilization of low-cost organic molecular and polymeric materials as the active layers in photovoltaic cells have attracted considerable attention [1–6]. In the past decade, low band-gap (LBG) organic molecules [7–12] and conjugated polymers [13–23] with internal electron donor–acceptor interaction have been developed and received continued interest towards highly efficient organic/polymeric solar cells. The donor–acceptor systems in the LBG polymers may cause partial intramolecular charge transfer (ICT) that enables manipulation of the electronic structure and provides the efficient charge separation of the photogenerated excitons. To date, the highest power conversion efficiencies of more than 5% have been achieved for solution processable organic polymer-based devices. The development of new materials that tune the molecular optical and electronic properties is still required with the aim to understand the intrinsic mechanism of conversion of sunlight into electric power, and to further improve the power conversion efficiency towards the practical application of organic solar cells.

Phthalocyanines (Pcs), as planar, two-dimensional aromatics, have emerged as a promising molecular component [24]. These macrocycles, alone or in combination with other electro- and photoactive moieties, have been ideal building blocks for the construction of molecular materials with designed electronic and optical properties [25]. The application of phthalocyanines into photovoltaic devices is usually performed in blends together with semiconductor polymers and/or acceptor molecules such as fullerenes via vapor deposition technique [26–32]. While examples based on solution processed bulk heterojunction solar cells using metallophthalocyanine complexes are scarce and the corresponding power conversion efficiencies are still low compared with that of polymer solar cells [33,34]. In our previous research, we developed an electron-accepting 2,1,3-benzothiadiazole-cored oligoalkylthiophene conjugates by a divergent synthetic method, and series of low band-gap polythiophene derivatives were prepared and their photovoltaic properties were studied [35,36]. In this paper, a hybrid of four low band-gap donor–acceptor moieties of 2,1,3-benzothiadiazole-cored oligoalkylthiophene conjugates and zinc phthalocyanine (denoted as **ZnPc-TDA** herein) was designed and synthesized (for structure, see Fig. 1). The central zinc phthalocyanine has high extinction coefficiency at around 700 nm, corresponding to the photo flux of solar spectrum, as well as excellent hole-transport ability. Four additional photoactive donor–acceptor conjugates were peripherally attached by ether linkage with the aim to cover the spectral window between 400 and 600 nm, where the **ZnPc** exhibit almost no absorption [37]. In this way, both broad absorption and good solubility were achieved [38]. Additionally, the combination of two separate components within one molecule provides a multiple pathway for electronic communications in the

* Corresponding authors. Tel.: +86 431 85098681; fax: +86 431 85098768.
E-mail addresses: liangfs112@nenu.edu.cn (F. Liang), xiezy_n@ciac.jl.cn (Z. Xie).

0927-0248/$ - see front matter © 2010 Elsevier B.V. All rights reserved.
doi:10.1016/j.solmat.2010.05.050

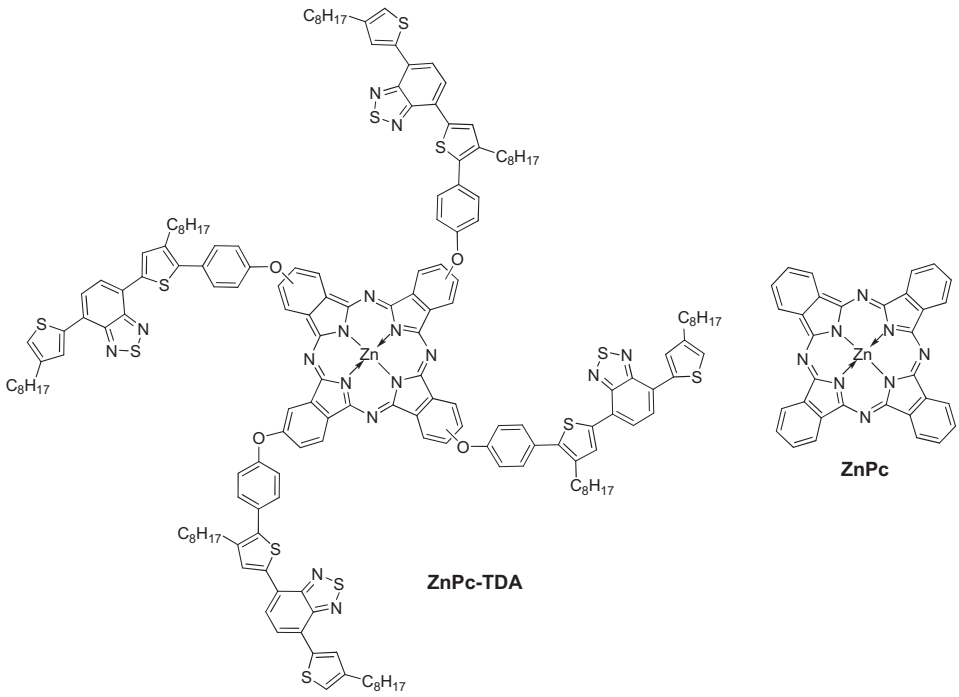

Fig. 1. Chemical structures of **ZnPc** and **ZnPc-TDA** reported herein.

assembled solar cells. To our best knowledge, phthalocyanine-based multicomponent systems have been explored, including perylenediimide [37], ferrocenes [39], tetrathiafulvalenes [40], dendrimers [41], C_{60} [25], thienyls [42], fluorenyl [43], and π-conjugated oligo(p-phenylenevinylene)s [44]. However, research on the low band-gap organic molecules functionalized metallophthalocyanines has not been reported.

2. Experimental section

2.1. Synthesis

Compounds 1–3 were prepared according to procedures in the literature [35,36].

Synthesis 4: Compound **3** (2.10 g, 4 mmol) and NBS (0.712 g, 4 mmol) were dissolved in 10 mL of CH_2Cl_2. The mixture was stirred at room temperature for 6 h, and then extracted with CH_2Cl_2 (3×10 mL), and dried over $MgSO_4$. Evaporation of the solvent gave 2.37 g (98% yield) of **4** as a red solid without further purification. ^{1}H NMR (500 MHz, $CDCl_3$) δ (ppm): 7.98 (s, 1H), 7.81 (d, J=7.5 Hz, 1H), 7.76 (s, 1H), 7.74 (d, J=7.5 Hz, 1H), 7.04 (s, 1H), 2.69 (t, 2H), 2.64 (t, 2H), 1.71–1.64 (m, 4H), 1.43–1.25 (m, 20H), 0.88 (t, 6H). ^{13}C NMR (125 MHz, $CDCl_3$) δ (ppm): 151.94, 142.93, 138.36, 127.87, 124.97, 124.50, 111.53, 31.88, 29.75, 29.63, 29.40, 29.31, 29.28, 27.81, 26.83, 22.67, 17.47, 14.13, 13.61. Elemental analysis calcd for $C_{30}H_{39}BrN_2S_3$: C, 59.68; H, 6.51; N, 4.64. Found: C, 59.85; H, 6.39; N, 4.62. MS calcd m/z 604.14. Found 605.15 $[(M+1)]^+$.

Synthesis 5: Compound **4** (1.81 g, 3 mmol), 4-hydroxyphenylboronic acid (0.61 g, 4.5 mmol), $Pd(PPh_3)_4$ (174 mg), and 2 M aqueous K_2CO_3 (20 mL) were added to the reaction vessel, which was vacuumed and flushed with nitrogen. THF (50 mL) were degassed with nitrogen and added via syringe. The reaction mixture was heated to reflux and stirred for 24 h under a nitrogen atmosphere. Then the reaction mixture was extracted with CH_2Cl_2 (3×10 mL). The combined organic phase was washed with water (3×20 mL), dried over $MgSO_4$, filtered and concentrated in vacuum. The crude product was purified by column chromatography on silica gel using petroleum ether and ethyl ether (20:1 V/V) as the eluent to give 0.95 g (51% yield) of **5** as a dark-red solid. ^{1}H NMR (500 MHz, $CDCl_3$) δ (ppm): 7.98 (d, 2H), 7.84 (s, 2H), 7.40 (d, J=8.5 Hz, 2H), 7.04 (s, 1H), 6.91 (d, J=8.5 Hz, 2H), 4.81 (s, 1H), 2.70 (t, 4H), 1.72–1.67 (m, 4H), 1.39–1.25 (m, 20H), 0.87 (t, 6H). ^{13}C NMR (125 MHz, $CDCl_3$) δ (ppm): 155.15, 152.55, 152.50, 144.29, 139.28, 138.99, 136.52, 130.60, 130.09, 128.86, 127.00, 125.73, 125.66, 125.49, 125.00, 121.38, 115.46, 31.88, 31.86, 30.99, 30.63, 30.48, 29.77, 29.69, 29.65, 29.55, 29.46, 29.39, 29.29, 29.27, 28.82, 22.67, 14.11. Elemental analysis calcd for $C_{36}H_{44}N_2OS_3$: C, 70.09; H, 7.19; N, 4.54. Found: C, 70.23; H, 7.02; N, 4.56. MS calcd m/z 616.26. Found 617.26 $[(M+1)]^+$.

Synthesis 6: 4-nitrophthalonitrile (0.26 g, 1.5 mmol) and **5** (0.93 g, 1.5 mmol) were dissolved in 10 mL of DMSO. After the reaction mixture was stirred for 15 min, $LiOH\cdot H_2O$ (0.16 g, 3.8 mmol) was added over 20 min, and the mixture was stirred for 15 h at room temperature. Then the reaction mixture was extracted with CH_2Cl_2 (3×10 mL). The combined organic phase was washed with water (3×20 mL), dried over $MgSO_4$, filtered and concentrated in vacuum. The crude product was purified by column chromatography on silica gel using petroleum ether and ethyl ether (40:1 V/V) as the eluent to give 0.93 g (83% yield) of **6** as a red solid. ^{1}H NMR (500 MHz, $CDCl_3$) δ (ppm): 8.01 (s, 1H), 7.99 (s, 1H), 7.85 (s, 2H), 7.75 (d, J=9 Hz, 1H), 7.61 (m, 2H), 7.37 (s, 1H), 7.31 (m, 1H), 7.15(m, 2H), 7.05 (s, 1H), 2.75 (t, 2H), 2.69 (t, 2H), 1.75–1.68 (m, 4H), 1.41–1.26 (m, 20H), 0.88 (t, 6H). ^{13}C NMR (125 MHz, $CDCl_3$) δ (ppm): 161.45, 152.86, 152.52, 152.49, 144.37, 140.15, 138.83, 137.66, 137.63, 135.41, 132.65, 131.32, 129.96, 129.05, 126.13, 125.40, 125.29, 121.66, 121.63, 121.49, 120.62, 117.67, 115.29, 114.87, 109.02, 31.84, 31.81, 30.95, 30.59, 30.46, 29.50, 29.41, 29.36, 29.33, 29.24, 29.21, 28.84, 22.62, 14.08. Elemental analysis calcd for $C_{44}H_{46}N_4OS_3$: C, 71.12; H, 6.24; N, 7.54. Found: C, 71.34; H, 6.04; N, 7.56. MS calcd m/z 742.28. Found 743.28 $[(M+1)]^+$.

Synthesis ZnPc-TDA: Compound **6** (594 mg, 0.8 mmol), $Zn(OAc)_2\cdot2H_2O$ (42.6 mg, 0.2 mmol), and 0.4 mL DBU were dissolved in 4 mL of 1-pentanol at nitrogen atmosphere. Under

stirring, the reaction mixture was heated to 140 °C for 24 h. After the mixture was cooled down, it was poured into 40 mL methanol, giving greenish dark solid. The solid was collected and purified by column chromatography on silica gel using petroleum ether and ethyl ether (2:1 V/V) as the eluent to give 0.37 g (61% yield) of **ZnPc-TDA** as a black solid. ^{1}H NMR (500 MHz, $CDCl_3$) δ (ppm): 7.68 (b, 40H), 6.83 (b, 8H), 2.56 (b, 16H), 1.57 (b, 16H), 1.27 (b, 80H), 0.84 (b, 24H). ^{13}C NMR (125 MHz, $CDCl_3$) δ (ppm): 158.25, 156.26, 151.88, 143.97, 139.22, 138.68, 138.15, 136.69, 130.40, 128.53, 124.75, 120.92, 119.41, 110.95, 31.93, 30.88, 30.55, 30.34, 29.72, 29.52, 29.37, 29.08, 22.71, 14.16. ^{1}IR (KBr): ν (cm^{-1}) 2952, 2922, 2851, 1599, 1503, 1488, 1394, 1335, 1233, 1090, 1044. Elemental analysis calcd for $C_{176}H_{184}N_{16}O_4S_{12}Zn$ (3033.06): C, 69.59; H, 6.11; N, 7.38. Found: C, 69.32; H, 6.02; N, 7.29. MALDI TOF-MS *m*/*z*: 3033.05.

2.2. Device fabrication

The photovoltaic devices were prepared by spin coating EL-grade PEDOT:PSS [poly (3,4-ethylene-dioxythiophene) polystyrenesulfonate] (Clevios P VPAI4083; H.C. Starck) onto cleaned, patterned indium tin oxide (ITO) substrates (14 $\Omega\,cm^{-2}$). The photoactive layer was deposited by spin coating from a chlorobenzene solution with a total concentration of 25 mg/mL. Film thicknesses were determined by profilometry (Veeco Dektak 150). The counter electrode of LiF (1 nm) and aluminum (100 nm) was deposited by vacuum evaporation at around 1×10^{-6} mbar. The active area of the cells was 0.167 cm^2. Spectral response was measured with a Keithley 2400 source meter, using monochromatic light from a tungsten–halogen lamp in combination with monochromator (Oriel, Cornerstone 130). A calibrated Si cell was used as reference. The device was kept behind a quartz window in a nitrogen filled container. *J–V* characteristics were measured under ca. 100 mW/cm^2 simulated solar light from a tungsten–halogen lamp (Philips Brilliantline Pro) filtered by a Schott GG 385 and a Hoya LB 120 filter. The exact current density was calculated by convolution of the spectral response with the AM1.5G spectrum (100 mW/cm^2).

3. Results and discussion

3.1. Synthesis

The synthetic route towards **ZnPc-TDA** was depicted in Scheme 1. The phthalonitrile ligand bearing a donor–acceptor motif **6** was obtained by sequential NBS monobromination of 4,7-bis(4-octylthiophen-2-yl)benzo[*c*][1,2,5]thiadiazole **3**, Suzuki coupling, and substitution reactions. The final zinc phthalocyanine **ZnPc-TDA** was successfully prepared by reacting compound **6** with $Zn(OAc)_2\cdot H_2O$ in reflux n-pentanol using DBU as the base, followed by column chromatographic purification on silica gel. The product was obtained as black powder and was characterized by ^{1}H NMR, IR spectroscopy and TOF-MS. The mass spectrum of **ZnPc-TDA** is shown in Fig. 2. **ZnPc-TDA** exhibited satisfactory solubility in common organic solvents such as $CHCl_3$, chlorobenzene, and dichlorobenzene, presumably due to the introduction of eight octyl chains on the donor–acceptor segments.

3.2. Absorption properties

The absorption spectra of **ZnPc-TDA** in $CHCl_3$ solution is shown in Fig. 3. (The absorption spectrum of **ZnPc** was also included for comparison.) The absorption peaks located at 332 and 696 nm with a shoulder peak at 634 nm were attributed to Q- and B-bands absorption of **ZnPc**, respectively [45]. The absorption maximum centered at 480 nm was derived from the intramolecular charge-transfer (ICT) transition of donor–accepter segments attached on the central zinc phthalocyanine [35,46]. The **ZnPc-TDA** film showed more intense, broader, and slightly red-shifted absorption than that in solution. A large coverage of the solar spectrum from UV to near IR region rendered it an ideal light-harvesting material in organic solar cells.

3.3. Thermal properties

The thermal property of **ZnPc-TDA** was investigated by DSC and TGA. **ZnPc-TDA** exhibited a melting peak at approx. 206 °C in

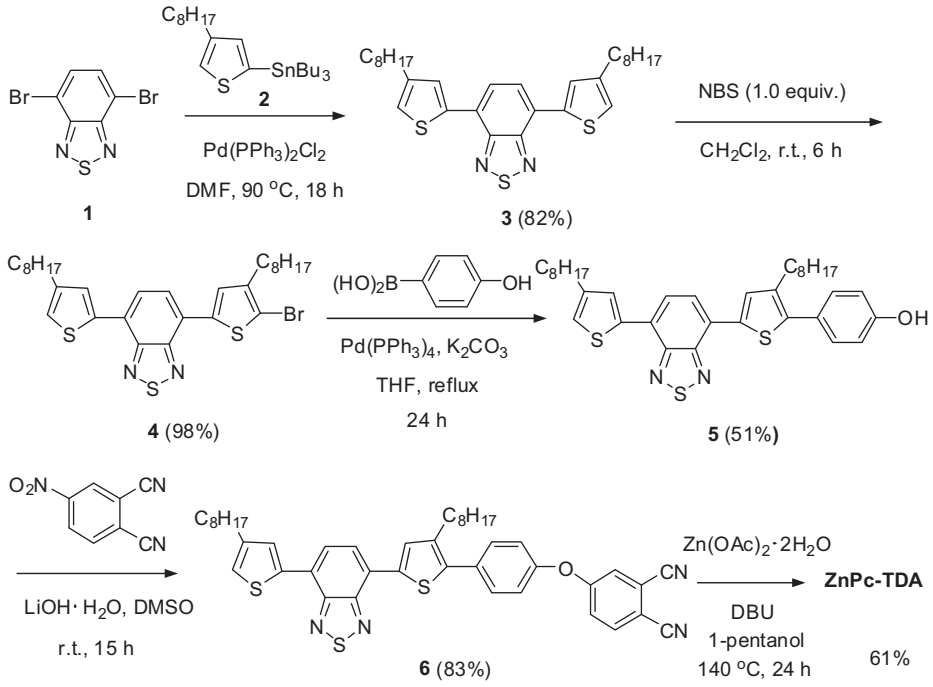

Scheme 1. Synthetic route towards donor–acceptor motif-containing zinc phthalocyanine **ZnPc-TDA**.

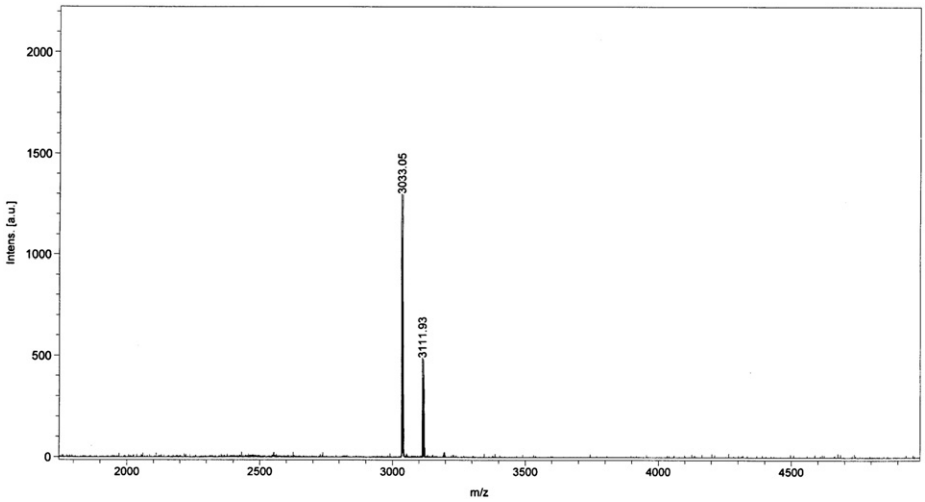

Fig. 2. Mass spectrum of **ZnPc-TDA.**

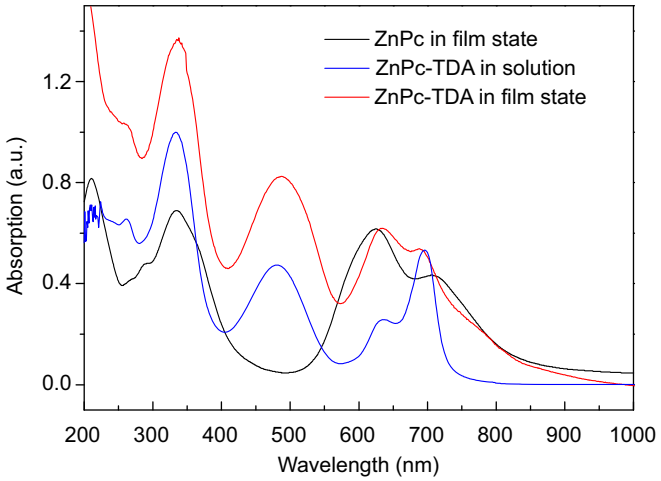

Fig. 3. UV–vis absorption spectra of **ZnPc** and **ZnPc-TDA** in solution (10^{-6} M) and in film state (spectra normalized at the longer-wavelength absorption maximum).

the heating curve. A weak crystallization peak at 171 °C was observed in the cooling curve, indicating that the material has a tendency to crystallize. TGA showed that **ZnPc-TDA** is thermally stable with only about 5% weight loss at 403 °C under N_2. The fundamental physical properties of **ZnPc-TDA** are summarized in Table 1.

3.4. Electrochemical properties

Cyclic voltammetry measurement of **ZnPc-TDA** was carried out under argon in a three-electrode cell using 0.1 M Bu_4NClO_4 in anhydrous CH_2Cl_2 as the supporting electrolyte. The CV curves were recorded referenced to an Ag quasi-reference electrode, which was calibrated using a ferrocene–ferrocenium (Fc/Fc^+) redox couple (4.8 eV below the vacuum level) as an external standard. The $E_{1/2}$ of the Fc/Fc^+ redox couple was found to be 0.40 V vs the Ag quasi-reference electrode. The CV curves of **ZnPc-TDA** in 0.1 M Bu_4NClO_4 solution in CH_2Cl_2 at a scan rate of 100 mV/s are shown in Fig. 4. Oxidation peaks corresponding to phthalocyanine and thiophene units could be observed upon positive scanning at 0.73 and 1.39 V, respectively. The reduction peak at −1.72 V was attributed to the thiophene segments and the reduction peak at −1.38 V was assigned to the electron-withdrawing benzothiadiazole moiety [35,36]. The HOMO and

Table 1
Physical properties of **ZnPc-TDA**.

λ_{max}^{abs}/nm ($10^{-5}\varepsilon_{max}/M^{-1}\,cm^{-1}$)[a]	332 (25.1), 480 (11.9), 696 (13.5)
E_{red}; E_{ox}/V[b]	−1.38, −1.72; 0.73, 1.39
HOMO, LUMO (eV)[c]	−4.91, −3.40
E_g^{Od}/E_g^{Ee} (eV)	1.63, 1.51
T_m[f],T_d[g] (°C)	206, 403

[a] Measured in $CHCl_3$.
[b] Determined by CV.
[c] Calculated from onset potentials.
[d] Optical energy gap estimated from the absorption edge of **ZnPc-TDA** solution.
[e] Energy gap = HOMO–LUMO.
[f] Determined by DSC at a heating rate of 10 °C min^{-1} under N_2.
[g] 5 wt% loss temperature, determined by TGA with a heating rate of 10 °C min^{-1} under N_2.

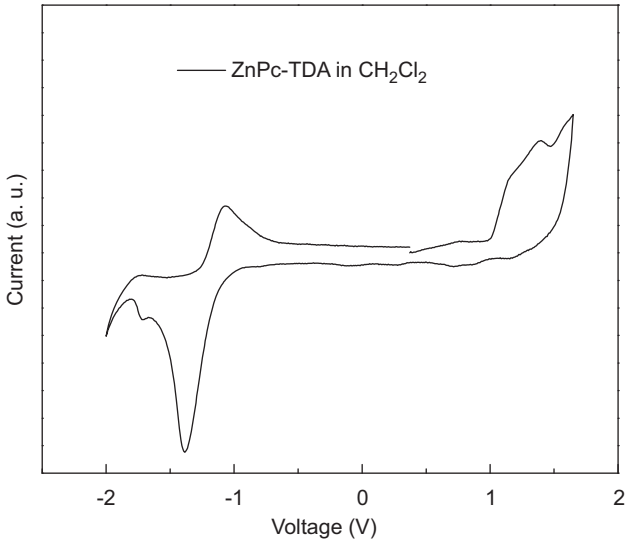

Fig. 4. CV curves of **ZnPc-TDA** in 0.1 M Bu_4NClO_4 solution in CH_2Cl_2 at a scan rate of 100 mV/s.

LUMO energy levels of **ZnPc-TDA** were estimated to be −4.91 and −3.40 eV using the empirical equation $E_{HOMO} = -(E_{ox}^{on} + 4.40)$ eV and $E_{LUMO} = -(E_{red}^{on} + 4.40)$ eV, respectively (E_{ox}^{on} and E_{red}^{on} stand for

the onset potentials for oxidation and reduction relative to the Ag quasi-reference electrode, respectively) [47].

3.5. Photovoltaic performances

As separate photoactive components, donor–acceptor thiophene-benzothiadiazole segments and metallophthalocyanine units have never been incorporated in the form of a single molecule such as **ZnPc-TDA**. To explore the **ZnPc-TDA** ensemble performance, solar cells with the configuration of ITO/PEDOT:PSS/**ZnPc-TDA**:PCBM/LiF/Al were fabricated using solution processible method. Chlorobenzene was selected as the solvent to spin-coat a blend of **ZnPc-TDA**:PCBM (1:*x*, wt/wt ratio, $x=1$, 2, 3, and 4) onto PEDOT:PSS pre-coated ITO substrates. It was observed that the increase of the amount of PCBM leads to the increase of the short circuit current density, while the open-circuit voltage gives no significant change. The **ZnPc-TDA**:PCBM (1:4) device exhibited relatively good power conversion efficiency. The thickness of **ZnPc-TDA**:PCBM (1:4) film was then optimized and the device performances were further improved (Table 2). The solar cell with the film thickness of 70 nm gave a power conversion efficiency of 0.42%. The current density–voltage characteristics of ITO/PEDOT:PSS/**ZnPc-TDA**:PCBM (1:4)/LiF/Al solar cells under AM 1.5 simulated solar illumination of 100 mW/cm^2 are shown in Fig. 5 and the corresponding and the EQE spectra are shown in Fig. 6. The preliminary solar cell data are similar to or lower than the metallophthalocyanines/porphyrins based solution-processed heterojunction solar cells reported in literatures [33,34,48–50]. The low power conversion efficiency may be explained as that the introduction of the peripheral substituent **TDA** onto the macrocycle of **ZnPc**, although the light-harvesting and charge-separation abilities were enhanced, might destroy the efficient π–π stacking between metallophthalocyanine molecules, which is obviously undesired for the solar cells. Hence, further modification of the molecular structure, for example, the introduction of organic segments into the metallophthalocyanine by a conjugated linkage, instead of the ether linkage, should be considered in the future work.

Table 2
Performance of the solution processed ITO/PEDOT:PSS/**ZnPc-TDA**:PCBM (1:4)/LiF/Al solar cells with different film thickness.[a,b]

Thickness (nm)	J_{sc} (mA cm^{-2})	V_{oc} (V)	*FF*	*PCE* (%)
200	0.84	0.64	0.26	0.14
115	1.08	0.64	0.25	0.17
90	1.81	0.63	0.27	0.31
70	2.26	0.68	0.28	0.42
50	1.67	0.62	0.26	0.27

[a] Under simulated AM 1.5 solar illumination at an irradiation intensity of 100 mW/cm^2.
[b] For as fabricated device.

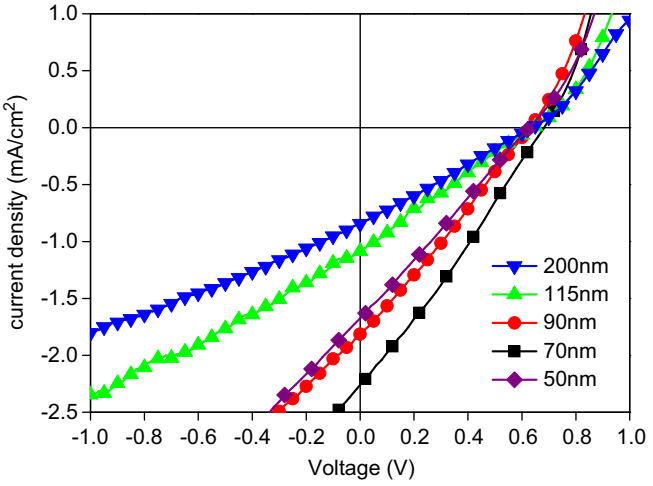

Fig. 5. Current density–voltage characteristics of ITO/PEDOT-PSS/**ZnPc-TDA**:PCBM (1:4) /LiF/Al solar cells with different film thickness under AM 1.5 simulated solar illumination of 100 mW/cm^2.

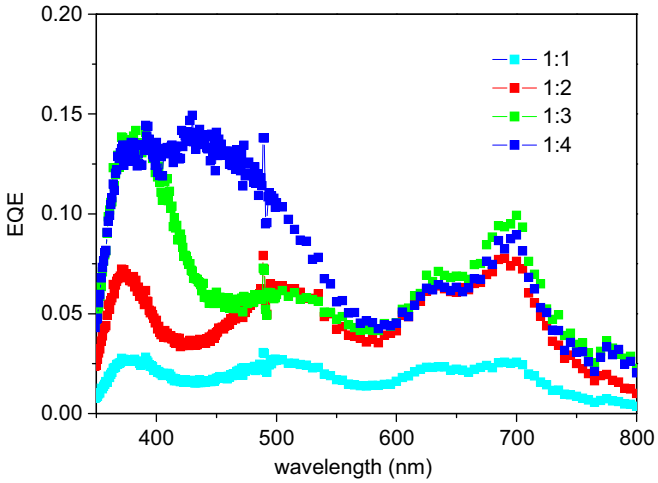

Fig. 6. EQE spectra of **ZnPc-TDA** based devices under AM 1.5 simulated solar illumination of 100 mW/cm^2.

4. Conclusions

We have synthesized the first zinc phthalocyanine with peripherally functionalized donor–acceptor conjugates through chemical linkage. The ensemble creates a new entry to realize a large coverage of the solar spectrum broad absorption, which corresponds to the sum of the absorption of the individual components. The application of such black zinc phthalocyanine in solution processible organic solar cells has been demonstrated, although the PCEs need to be improved.

Acknowledgments

This work was supported by NSFC (20703008 and 20972027), MOST of China (2009CB623605), the Department of Science and Technology of Jilin Province (20080421), Training Fund of NENU'S Scientific Innovation Project (NENU-STC08013) and Analysis and Testing Foundation of Northeast Normal University.

References

[1] G. Yu, J. Gao, J.C. Hummelen, F. Wudl, A.J. Heeger, Polymer photovoltaic cells: enhanced efficiencies via a network of internal donor–acceptor heterojunctions, Science 270 (1995) 1789–1791.
[2] K.M. Coakley, M.D. McGehee, Conjugated polymer photovoltaic cells, Chem. Mater. 16 (2004) 4533–4542.
[3] C.J. Brabec, N.S. Sariciftci, J.C. Hummelen, Plastic solar cells, Adv. Funct. Mater. 11 (2001) 15–26.
[4] S. Gunes, H. Neugebauer, N.S. Sariciftci, Conjugated polymer-based organic solar cells, Chem. Rev. 107 (2007) 1324–1338.
[5] M. Helgesen, R. Søndergaard, F.C. Krebs, Advanced materials and processes for polymer solar cell devices, J. Mater. Chem. 20 (2010) 36–60.
[6] F.C. Krebs, T.D. Nielsen, J. Fyenbo, M. Wadstrøm, M.S. Pedersen, Manufacture, integration and demonstration of polymer solar cells in a lamp for the "Lighting Africa" initiative, Energy Environ. Sci. 3 (2010) 512–525.

[7] H.Y. Chen, J. Hou, S. Zhang, Y. Liang, G. Yang, Y. Yang, L. Yu, Y. Wu, G. Li, Polymer solar cells with enhanced open-circuit voltage and efficiency, Nat. Photon. 3 (2009) 649–653.
[8] K. Schulze, C. Uhrich, R. Schüppel, K. Leo, M. Pfeiffer, E. Brier, E. Reinold, P. Bäuerle, Efficient vacuum-deposited organic solar cells based on a new low-bandgap oligothiophene and fullerene C_{60}, Adv. Mater. 18 (2006) 2872–2875.
[9] T.M. Pappenfus, M.W. Burand, D.E. Janzen, K.R. Mann, Synthesis and characterization of tricyanovinyl-capped oligothiophenes as low-band-gap organic materials, Org Lett. 5 (2003) 1535–1538.
[10] P. Suresh, P. Balraju, G.D. Sharma, J.A. Mikroyannidis, M.M. Stylianakis, Effect of the incorporation of a low-band-gap small molecule in a conjugated vinylene copolymer: PCBM blend for organic photovoltaic devices, ACS Appl. Mater. interfaces 1 (2009) 1370–1374.
[11] A.B. Tamayo, B. Walker, T.Q. Nguyen, A. Low Band, Gap, solution processable oligothiophene with a diketopyrrolopyrrole core for use in organic solar cells, J. Phys. Chem. C 112 (2008) 11545–11551.
[12] X. Li, A. Liu, S. Xun, W. Qiao, X. Wan, Z.Y. Wang, Synthesis and characterization of near-infrared absorbing and fluorescent liquid-crystal chromophores, Org. Lett. 10 (2008) 3785–3787.
[13] G. Qian, Z. Zhong, M. Luo, D. Yu, Z. Zhang, Z.Y. Wang, D. Ma, Simple and efficient near-infrared organic chromophores for light-emitting diodes with single electroluminescent emission above 1000 nm, Adv. Mater. 21 (2009) 111–116.
[14] F. Zhang, W. Mammo, L.M. Andersson, S. Admassie, M.R. Andersson, O. Inganäs, Low-bandgap alternating fluorene copolymer/methanofullerene heterojunctions in efficient near-infrared polymer solar cells, Adv. Mater. 18 (2006) 2169–2173.
[15] F. Wang, J. Luo, K. Yang, J. Chen, F. Huang, Y. Cao, Conjugated fluorene and silole copolymers: synthesis, characterization, electronic transition, light emission, photovoltaic cell, and field effect hole mobility, Macromolecules 38 (2005) 2253–2260.
[16] N. Blouin, A. Michaud, M. Leclerc, A low-bandgap poly(2,7-carbazole) derivative for use in high-performance solar cells, Adv. Mater. 19 (2007) 2295–2300.
[17] C. Winder, N.S. Sariciftci, Low bandgap polymers for photon harvesting in bulk heterojunction solar cells, J. Mater. Chem. 14 (2004) 1077–1086.
[18] E. Bundgaard, F.C. Krebs, Low band gap polymers for organic photovoltaics, Sol. Energy Mater. Sol. Cells 91 (2007) 954–985.
[19] Z. Zhu, D. Waller, R. Gaudiana, M. Morana, D. Mu1hlbacher, M. Scharber, C. Brabec, Panchromatic conjugated polymers containing alternating donor/acceptor units for photovoltaic applications, Macromolecules 40 (2007) 1981–1986.
[20] N. Blouin, A. Michaud, D. Gendron, S. Wakim, E. Blair, R. Neagu-Plesu, M. Belletete, G. Durocher, Y. Tao, M. Leclerc, Toward a rational design of poly(2,7-carbazole) derivatives for solar cells, J. Am. Chem. Soc. 130 (2008) 732–742.
[21] J.K. Lee, W.L. Ma, C.J. Brabec, J. Yuen, J.S. Moon, J.Y. Kim, K. Lee, G.C. Bazan, A.J. Heeger, Processing additives for improved efficiency from bulk heterojunction solar cells, J. Am. Chem. Soc. 130 (2008) 3619–3623.
[22] M.M. Wienk, M. Turbiez, J. Gilot, R.J.J. Janssen, Narrow-bandgap diketo-pyrrolo-pyrrole polymer solar cells: the effect of processing on the performance, Adv. Mater. 20 (2008) 2556–2560.
[23] A.P. Zoombelt, M. Fonrodona, M.M. Wienk, A.B. Sieval, J.C. Hummelen, R.A.J. Janssen, Photovoltaic performance of an ultrasmall band gap polymer, Org. Lett. 11 (2009) 903–906.
[24] G. de la Torre, C.G. Claessens, T. Torres, Phthalocyanines: old dyes, new materials. putting color in nanotechnology, Chem. Commun. 20 (2007) 2000–2015.
[25] G. Bottari, D. Olea, C. Gómez-Navarro, F. Zamora, J. Gómez-Herrero, T. Torres, Highly conductive supramolecular nanostructures of a covalently linked phthalocyanine–C_{60} fullerene conjugate, Angew. Chem. Int. Ed. 47 (2008) 2026–2031.
[26] I. Kim, H.M. Haverinen, Z. Wang, S. Madakuni, Y. Kim, J. Li, G.E. Jabbour, Efficient organic solar cells based on planar metallophthalocyanines, Chem. Mater. 21 (2009) 4256–4260.
[27] Y. Shao, Y. Yang, Efficient organic heterojunction photovoltaic cells based on triplet materials, Adv. Mater. 17 (2005) 2841–2844.
[28] J. Xue, B.P. Rand, S. Uchida, S.R. Forrest, A hybrid planar-mixed molecular heterojunction photovoltaic cell, Adv. Mater. 17 (2005) 66–71.
[29] I. Bruder, J. Schöneboom, R. Dinnebier, A. Ojala, S. Schäfer, R. Sens, P. Erk, J. Weis, What determines the performance of metal phthalocyanines (MPc, M=Zn,Cu, Ni, Fe) in organic heterojunction solar cells? A combined experimental and theoretical investigation, Org. Electron. 2009. doi:10.1016/j.orgel. 2009.11.016.
[30] D. Placencia, W. Wang, R.C. Shallcross, K.W. Nebesny, M. Brumbach, N.R. Armstrong, Organic photovoltaic cells based on solvent-annealed, textured titanyl phthalocyanine/C_{60} heterojunctions, Adv. Funct. Mater. 19 (2009) 1913–1921.
[31] M. Brumbach, D. Placencia, N.R. Armstrong, Titanyl phthalocyanine/C_{60} heterojunctions: band-edge offsets and photovoltaic device performance, J. Phys. Chem. C 112 (2008) 3142–3151.
[32] S. Pfuetzner, J. Meiss, A. Petrich, M. Riede, K. Leo, Thick C_{60}:ZnPc bulk heterojunction solar cells with improved performance by film deposition on heated substrates, Appl. Phys. Lett. 94 (2009) 253303.
[33] M.K.R. Fischer, I. López-Duarte, M.M. Wienk, M.V. Martínez-Díaz, R.A.J. Janssen, P. Bäuerle, T. Torres, Functionalized dendritic oligothiophenes: ruthenium phthalocyanine complexes and their application in bulk heterojunction solar cells, J. Am. Chem. Soc. 131 (2009) 8669–8676.
[34] F. Silvestri, I. López-Duarte, W. Seitz, L. Beverina, M.V. Martínez-Díaz, T.J. Marks, D.M. Guldi, G.A. Pagani, T. Torres, A squaraine–phthalocyanine ensemble: towards molecular panchromatic sensitizers in solar cells, Chem. Commun. 30 (2009) 4500–4502.
[35] J. Lu, F. Liang, N. Drolet, J. Ding, Y. Tao, R. Movileanu, Crystalline low band-gap alternating indolocarbazole and benzothiadiazole-cored oligothiophene copolymer for organic solar cell applications, Chem. Commun. 42 (2008) 5315–5317.
[36] F. Liang, J. Lu, J. Ding, Y. Tao, Design and synthesis of alternating regioregular oligothiophenes/benzothiadiazole copolymers for organic solar cells, Macromolecules 42 (2009) 6107–6114.
[37] X. Li, L.E. Sinks, B. Rybtchinski, M.R. Wasielewski, Ultrafast aggregate-to-aggregate energy transfer within self-assembled light-harvesting columns of zinc phthalocyanine tetrakis (perylenediimide), J. Am. Chem. Soc. 126 (2004) 10810–10811.
[38] Y. Li, Y. Zou, Conjugated polymer photovoltaic materials with broad absorption band and high charge carrier mobility, Adv. Mater. 20 (2008) 2952–2958.
[39] K.W. Poon, Y. Yan, X. Li, D.K.P. Ng, Synthesis and electrochemistry of ferrocenylphthalocyanines, Organometallics 18 (1999) 3528–3533.
[40] C. Farren, C.A. Christensen, S. FitzGerald, M.R. Bryce, A. Beeby, Synthesis of novel phthalocyanine – tetrathiafulvalene hybrids; intramolecular fluorescence quenching related to molecular geometry, J. Org. Chem. 67 (2002) 9130–9139.
[41] M. Brewis, G.J. Clarkson, M. Helliwell, A.M. Holder, N.B. McKeown, The synthesis and glass-forming properties of phthalocyanine-containing poly(aryl ether) dendrimers, Chem. Eur. J. 6 (2000) 4630–4636.
[42] T. Muto, T. Temma, M. Kimura, K. Hanabusa, H. Shirai, Elongation of the π-system of phthalocyanines by introduction of thienyl substituents at the peripheral β positions. synthesis and characterization, J. Org. Chem. 66 (2001) 6109–6115.
[43] C.A. Barker, X. Zeng, S. Bettington, A.S. Batsanov, M.R. Bryce, A. Beeby, Porphyrin, phthalocyanine and porphyrazine derivatives with multifluorenyl substituents as efficient deep-red emitters, Chem. Eur. J. 13 (2007) 6710–6717.
[44] M. Kimura, H. Narikawa, K. Ohta, K. Hanabusa, H. Shirai, N. Kobayashi, Star-shaped stilbenoid phthalocyanines, Chem. Mater. 14 (2002) 2711–2717.
[45] Y. Luo, J. Gao, C. Cheng, Y. Sun, X. Du, G. Xu, Z. Wang, Fabrication micro-tube of substituted Zn–phthalocyanine in large scale by simple solvent evaporation method and its surface photovoltaic properties, Org. Electron. 9 (2008) 466–472.
[46] J. Subbiah, P.M. Beaujuge, K.R. Choudhury, S. Ellinger, J.R. Reynolds, F. So, Efficient green solar cells via a chemically polymerizable donor – acceptor heterocyclic pentamer, ACS Appl. Mater. Interfaces 1 (2009) 1154–1158.
[47] J. Pommerehne, H. Vestweber, W. Guss, R.F. Mahrt, H. Bassler, M. Porsch, J. Daub, Efficient two layer leds on a polymer blend basis, Adv. Mater. 7 (1995) 551–554.
[48] O. Hagemann, M. Jørgensen, F.C. Krebs, Synthesis of an all-in-one molecule (for organic solar cells), J. Org. Chem. 71 (2006) 5546–5559.
[49] F.C. Krebs, H. Spanggaard, Sol. Energy Mater. Sol. Cells 88 (2005) 363–375.
[50] F.C. Krebs, O. Hagemann, M. Jørgensen, Sol. Energy Mater. Sol. Cells 83 (2004) 211–228.